

Dynamical investigation of the multiple star ADS 9173 AB

O.V. Kiyaveva^{*1}, I.S. Izmailov¹, N.V. Narizhnaya¹, L.G. Romanenko¹

¹The Central Astronomical Observatory of the Russian Academy of Sciences at Pulkovo

July 2023

Abstract

Star ADS 9173=WDS 14135+5147=Hip 69483 is a complex system. The B component has a spectroscopic companion, whose orbit with a period of 4.9 years has been known since 1986. The Gaia telescope has detected a distant faint pair over 100" away from the bright AB pair. In our article, we study the movement in a bright pair based on long-term observations with the 26-inch refractor of the Pulkovo Observatory. The AB pair orbit with a period of 6306 years was calculated using the apparent motion parameters (AMP) method. The astrometric orbit of the component B was determined on the basis of the residuals of the homogeneous CCD observations up to 2023 with the 26-inch refractor. It is in agreement with the spectroscopic one. The remaining secondary residuals show a wave with a period of approximately 20 years, the reasons for which are discussed.

Introduction

When studying the process of formation of stars and exoplanets, the further dynamic evolution of stellar groups and systems of exoplanets, it is important to pay attention to double and multiple systems. Observations in the optical to centimeter range indicate that multiple systems of two or more bodies are the norm throughout all stages of stellar evolution. It is widely accepted that multiple systems arise from the collapse and fragmentation of cloud cores, despite the inhibitory effect of magnetic fields. This fact is noted in many works on these topics (Bally et al., 2014). The search for multiple systems is therefore an urgent observational problem. Especially when it comes to studying exoplanet systems (Mugrauer, 2019).

Observation of double and multiple stars is a traditional topic for the Pulkovo Observatory since the days of W. Struve. Observations and a search for possible inner subsystems are currently ongoing with the 26-inch refractor (Zakhozhay et al., 2010; Grosheva, 2006; Kiyaveva et al., 2021). This article continues a series of ADS 9173 studies (Kiyaveva, 2006; Kiyaveva, Zhuchkov, 2017) based on photographic and CCD observations with a 26-inch refractor.

In the work (Kiyaveva, 2006) the preliminary orbit of the AB pair was determined for the first time by the AMP method on the basis of photographic observations in 1982–2004. Also an attempt was made to obtain astrometric orbit consistent with the spectroscopic orbit of the photocenter, using residuals. The spectroscopic orbit was derived from 70 years of radial velocity observations as early as 1986 (Bakos, 1986). From the spectroscopic orbit, 3 dynamic

*e-mail:kiyaveva@list.ru

parameters were adopted: period P , eccentricity e and the instant of the periastron passage T . The astrometric orbit allows you to determine the orientation of the orbit plane (the angle of inclination i and ascending node longitude Ω). Orbit matching is controlled by a common parameter independently obtained spectroscopically and astrometrically, the periastron longitude from the ascending node ω . The accuracy of the photographic observations was not sufficient to obtain reliable agreement, although the presence of a satellite in positional observations was noted. In addition, the perturbation in declination with a period of more than 13 years were discovered.

In the work (Kiyeva, Zhuchkov, 2017), based on photographic and CCD observations of 2003–2012, a preliminary orbit of a possible satellite with a period of 20 years was determined. At the same time, the motion of the AB pair in the 1982–2012 segment turned out perpendicular to the plane of the sky in the direction ρ , since $\dot{\theta} = 0.0002 \pm 0.0010 \approx 0^\circ/\text{year}$, which is not confirmed by 200-year observations. It was not possible to obtain a satisfactory orbit of the AB pair with such parameters of apparent motion.

At present, the Gaia telescope has discovered by the common parallax one more pair of weak stars ($m \approx 15^m$) Cab of low mass (see the MSC catalog (Tokovinin, 2018)) at a distance of $114''$. In the Gaia DR3 catalog (Gaia Collaboration, 2022) there are no parallax and proper motions for the B component due to low accuracy which is created by the inner subsystem, and there is also no radial velocity of the A component. Perhaps the reason for the lack of data is that the stars are bright, and there are problems with determining the radial velocities for stars of spectral type A (according to the WDS catalog (Mason et al., 2016): $m_A = 4.57^m$, $Sp_A = A7V$, $m_B = 6.81^m$, $Sp_B = F1V$).

In this work, the orbit of the AB pair is determined from the entire series of observations. From the residuals relative to this orbit the astrometric orbit of component B is determined. It consistent with the spectroscopic orbit within the error limits. The question of the reality of the second satellite with a period of 20 years, which manifests itself in residual deviations, is discussed.

1 Observations

The bright pair ADS 9173 AB was discovered by William Herschel in 1779, but W. Struve’s 1832 observation (obtained by 7 separate positions) and O. Struve’s 1847 observation (obtained by 11 separate positions) are the most reliable early observations. among those included in the WDS catalog. There are only 192 observations in WDS (2016 version) for 1779–2015. During this time, the distance between the components has changed only by $1''$, and the position angle by 1° (see Fig. 1). To reduce the large scatter caused by the influence of possible inner subsystems, we averaged all observations in a sliding window of 20 years. After 2000, we took into account only our homogeneous observations. Later, to determine the orbit of the outer pair, we used this series 1831–2010 (62 positions).

The star has been observed at the Pulkovo Observatory with a 26-inch refractor since 1982. There are 48 photographic observations from 1982–2004 measured with a scanner (Kiselev et al., 2014), and 71 CCD observations from 2003–2019 (see Izmailov et al. (2020)). The last 13 CCD-observations for 2020–2023 are presented in this paper. A systematic difference between photographic and CCD-observations in ρ was found: Photo-CCD=50 mas. This correction has been introduced in the set of photographic observations. Comparison of the combined series

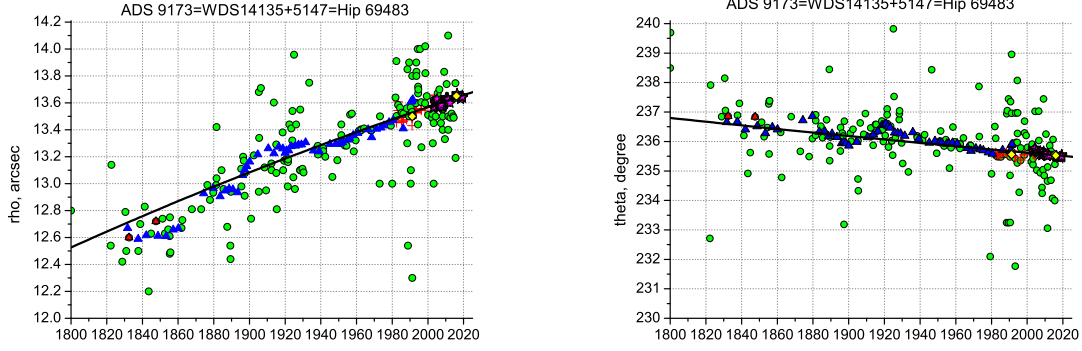


Figure 1: The entire series of the ADS 9173 AB observations. Designations: green circles indicate observations from WDS (Mason et al., 2016), blue triangles are smoothed series, the red triangles are the observations of Wilhelm and Otto Struve, yellow diamonds are space observations of Hipparcos (from WDS), Gaia DR2 (Gaia Collaboration et al., 2018) and Gaia DR3 (Gaia Collaboration, 2022), red crosses are Pulkovo photographic observations (Kiselev et al., 2014), magenta asterisks are CCDs (see Izmailov et al. (2020)), the line is the ephemeris of the wide pair AB orbit.

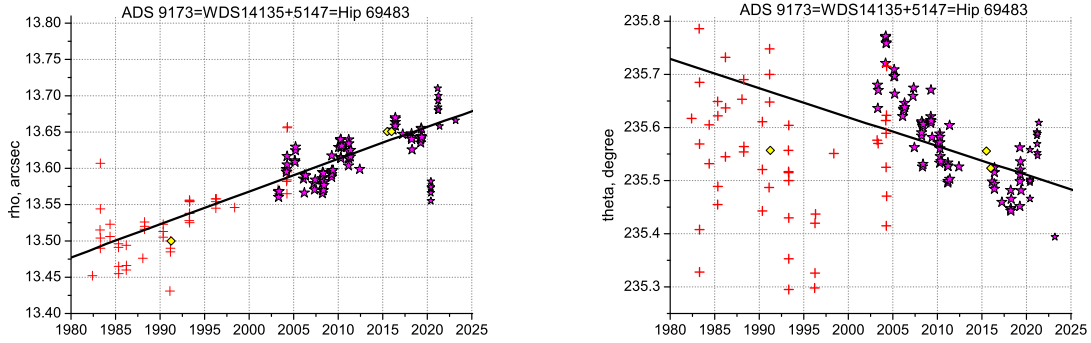


Figure 2: A series of observations on the Pulkovo 26-inch refractor. The designations are the same as in Fig. 1. Dependence $\theta(t)$ shows a disturbance with a period of about 20 years.

with the worldwide observations from the WDS did not reveal any systematic discrepancies.

All observations are shown in Fig. 1. The Pulkovo observations are presented separately in Fig. 2.

On the $\rho(t)$ graph, the smoothed series demonstrates a clearly pronounced wave in the 1830–1940 segment, however, it doesn't show up any further. This example of observational selection shows that one wave is not enough to confirm the astrometric orbit obtained from residuals, careful analysis of all available data is required.

2 AMP-orbit of the A-B pair

The AMP method (Kiselev, Kiyayeva, 1980) is designed to determine the initial orbits of wide visual binary stars with a long period of revolution in position and velocity at the one moment on the basis of the results of observations, obtained by various available methods. These are the apparent motion parameters (AMP) at the instant T_0 : the apparent distance between components (ρ), the position angle (θ), the apparent relative motion (μ), and the positional angle of direction of the relative motion (ψ), the radius of curvature (ρ_c).

In addition, the necessary data are the parallax p_t (for the relationship between linear and angular quantities), the relative radial velocity of the components ΔV_r obtained from spectroscopic observations (to calculate the spatial velocity vector of the satellite B relative to the main star A) and an estimate of the components mass sum ΣM according to the data on the physical properties of the stars.

If it is possible to determine all five parameters, including the radius of curvature, then the distance between the components r in astronomical units is calculated by the formula

$$r^3 = k^2 \frac{\rho \rho_c}{\mu^2} |\sin(\theta - \psi)| \quad (1)$$

where $k^2 = 4\pi^2 \Sigma M$ is a dynamic constant if distance is measured in AU, time in years, mass in solar mass units.

Then we get two position vectors that correspond to the position of the secondary component symmetrically with respect to the picture plane, and, consequently, two orbits, each of which is characterized by an angle β between the spatial position of the satellite and its projection onto the picture plane.

$$\beta = \pm \arccos \frac{\rho}{r p_t} \quad (2)$$

Both orbits have the same semi-major axes and periods, but other parameters differ.

Most precisely, the AMP are obtained from homogeneous observations (basis), performed on the same telescope in order to eliminate instrumental systematic errors. All other observations are used to control and, if necessary, to refine the unknown initial data.

In our case, as can be seen from Fig. 2, the most accurate is a series of CCD observations. However, the relative movement of the components is too slow, and it is impossible to get the parameters of the visible movement only on the basis of this homogeneous series, distorted by the influence of possible satellites. Therefore the AMPs are calculated for the moment 1950.0 over the entire smoothed series. The components mass sum we took from the MSC catalog. Unfortunately, it is impossible to determine the radius of curvature, and the relative radial velocity is determined uncertainly.

In the work (Bakos, 1986), $V_{rB\gamma} = -21.5$ km/s was determined for component B and $V_{rA} = -23$ km/s was approximately estimated. In agreement with the remote observations, we determined the angle $\beta = -11^\circ$ and refined $\Delta V_r = +1.7$ km/s. The smoothed observations of 1831–1940 and 2000–2010 were used as distant observations.

To select the best solution, we use an algorithm, proposed in the work (Kiyeva, 1983). In this algorithm observations and ephemeris are compared not directly, but the Thiele-Innes elements A, B, F, G, calculated in two ways: by the geometric elements of the AMP orbit (a, i, ω and Ω) and as a least-squares method solution of the system of linear equations, where, along with the observed coordinates, the dynamical elements of the AMP orbit (P, T and e) are used. Ideally, these values should match. We are looking for the minimum of the comparison function S depending on the difference of the Thiele-Innes elements.

$$S = (\Delta A^2 + \Delta B^2 + \Delta F^2 + \Delta G^2)^{1/2} \quad (3)$$

Dependences $S(\beta)$ and $S(\Delta V_r)$ are shown in Fig. 3.

According to this criterion, we confidently obtain the best solution corresponding to $\beta =$

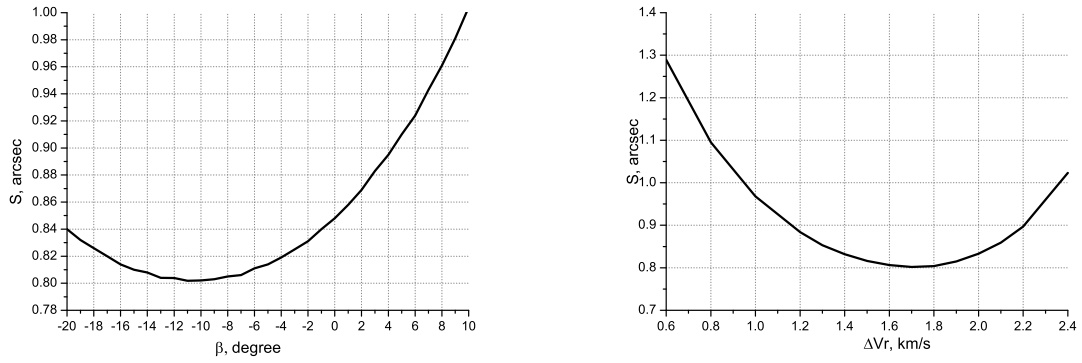


Figure 3: Dependences $S(\beta)$ and $S(\Delta V_r)$ for ADS 9173 AB.

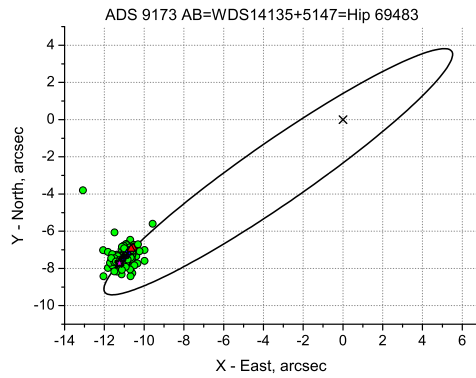


Figure 4: Orbit of the outer A-B pair in the picture plane. The oblique cross denotes the main component of A, the rest of the designations are the same as in Fig. 1.

$-11^\circ \pm 7^\circ$. If we use the minimum dispersion criterion over the entire series of observations, the second solution, corresponding to $\beta = +11^\circ$, also passes well through the entire series. However, when comparing the Thiele-Innes elements, we take into account not only positional observations, but also the elements of the AMP-orbit T and e , which are different for different solutions. Therefore, we believe that the only correct solution is the one corresponding to $\beta = -11^\circ$.

The initial data for obtaining the AMP-orbit are presented in Table 1, orbit elements - in Table 2.

Orbital element errors are determined by the total change of each element when changing all the initial parameters by the values of their errors. Since the resulting range of element values is not symmetrical with respect to the calculated parameter, we indicated the uncertainties in both directions. Fig. 4 shows the orbit of the outer pair in the picture plane.

Table 1: Initial data for determining the AMP orbit of the AB pair.

T_0 , yr	ρ ,''	θ , $^\circ$	μ , mas/yr	ψ , $^\circ$	ΔV_r , km/s	p_t , mas	ΣM , M_\odot
1950.0	13.335	235.897	5.029	220.70	+1.7	20.153	4.2
	± 0.010	± 0.023	± 0.193	± 1.28	± 0.2	± 0.009	

Table 2: Elements of the AMP orbit of the AB pair.

	$a, ''$	$P, \text{ yr}$	e	$\omega, ^\circ$	$i, ^\circ$	$\Omega, ^\circ$	$T, \text{ yr}$
	11.10	6306.	.44	208.0	99.2	234.1	6515.
+	1.56	1362.	.10	16.5	1.1	.2	119.
-	.96	800.	.19	16.6	1.4	1.7	611.

The second and third lines contain the uncertainties that define the range for each parameter.

3 Astrometric orbit of the inner Ba-Bb pair

To determine the astrometric orbit of component B, we use only CCD observations 2003–2023. During this time, the pair made 4 revolutions. The observations and (O-C) in right ascension (dx1) and in declination (dy1) relative to the orbit of the AB pair are presented in Table 3. The residuals dx1 and dy1 are the input data for calculating the astrometric Ba-Bb orbit. Observation weights are determined by the $Err\rho$ error.

The photocenter orbit is defined in a standard way. We solve the system of equations:

$$dx_{phase} = dx_0 + BX_{phase} + GY_{phase} \quad (4)$$

$$dy_{phase} = dy_0 + AX_{phase} + FY_{phase} \quad (5)$$

where dx_{phase} and dy_{phase} are the original residuals depending on the phase with respect to the period, which is equal to the fractional part of $(t - T_0)/P$; $X_{phase} = \cos(E_{phase}) - e$, $Y_{phase} = \sqrt{1 - e^2} \sin(E_{phase})$ are the orbital coordinates, depending on the orbital elements P, T and e , which in our case are known with high accuracy from the spectroscopic orbit (Bakos, 1986), E is the true anomaly at time t . Note that the instant of the periastron passage T is recalculated taking into account the fact that from 1927 to 2010 the star made 17 revolutions.

We determine the coordinates of the mass center dx_0 and dy_0 at the instant $T_0 = 2012.0$ and the elements Thiele-Innes A, B, F, G, which correspond to the elements of the orbit (a, i, ω, Ω) . The errors of these elements relative to the calculated solution were determined by the Monte Carlo method, the number of trials is 30, the initial residuals were distorted with an adopted dispersion of 15 mas, which corresponds to the accuracy of the CCD observations. These errors are slightly larger than those of the average solution, difference between model and average elements falls within this range.

The results are shown in Table 4 and in Fig. 5.

The residuals are averaged over the phase in a sliding window equal to $0.05P \approx 0.25$ years, the errors of each position are external and determine the convergence within the phase. Ephemeris of the inner pair Ba-Bb orbit in comparison with all initial data are also presented in Fig. 6.

The periastron longitude from the ascending node ω is determined independently from the spectroscopic and from the astrometric orbit, and therefore this parameter can be considered as a consistency control orbits. Within the error, the values of ω coincide. Thus, we have supplemented the spectroscopic orbit with the missing parameters i and Ω .

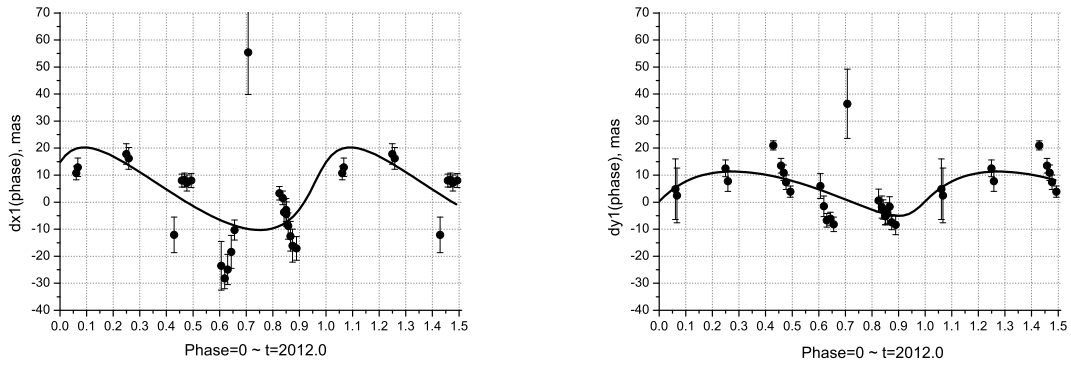


Figure 5: Comparison of Ba-Bb astrometric orbit ephemeris with phase-averaged residuals of CCD observations relative to AB orbit.

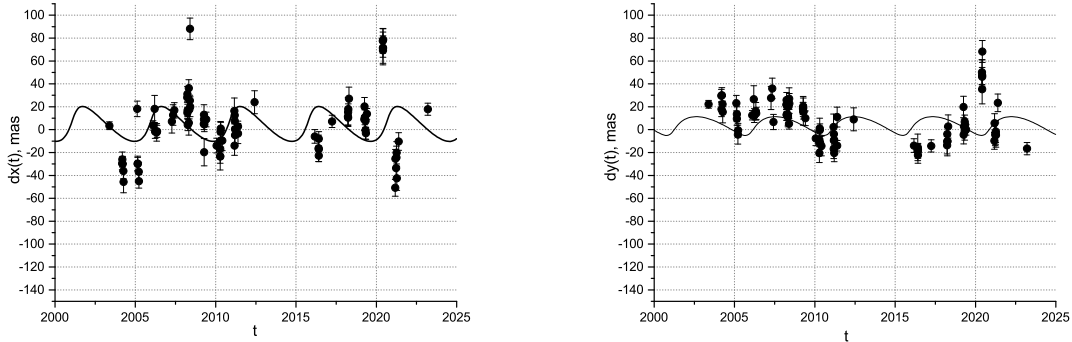


Figure 6: Comparison of the Ba-Bb astrometric orbit ephemeris with deviations of individual CCD observations relative to the AB orbit.

4 Is there another satellite in this system?

Let us consider the residuals of Pulkovo CCD observations. After taking into account the orbit of the outer AB pair mean square deviations $\sigma_x = 42.8$ mas, $\sigma_y = 42.5$ mas. After taking into account astrometric orbit of Ba-Bb, they have significantly decreased ($\sigma_x = 30.8$ mas, $\sigma_y = 19.1$ mas). These residuals (dx_2 , dy_2) are also presented in Table 3. Here, the weights of observations are not taken into account.

On Fig. 7, the deviations of Pulkovo photographic observations are also added to them after accounting for both orbits. It can be seen on the $dy_2(t)$ graph, that the move of photographic and CCD deviations is repeated in the time intervals 1985–1996 and 2005–2012. The characteristic trend allowed us to assume satellite presence with a period of approximately 20 years. Unfortunately, the star was rarely observed by photography after 1996, and 2012–2015 CCD observations are absent. Until 2019, CCD-observations do not contradict this assumption, but the latest observations are 2020, 2021 and 2023 made us doubt.

In addition, in Fig. 5, we see that the positions near close phases differ from the natural random spread and indicate some systematic movement.

Therefore, we have now come to the conclusion that the system has a short-period satellite (perhaps more than one) that we cannot confidently detect, and the 20-year period is caused by observational selection or is a multiple for several satellites. Compared to our Solar system,

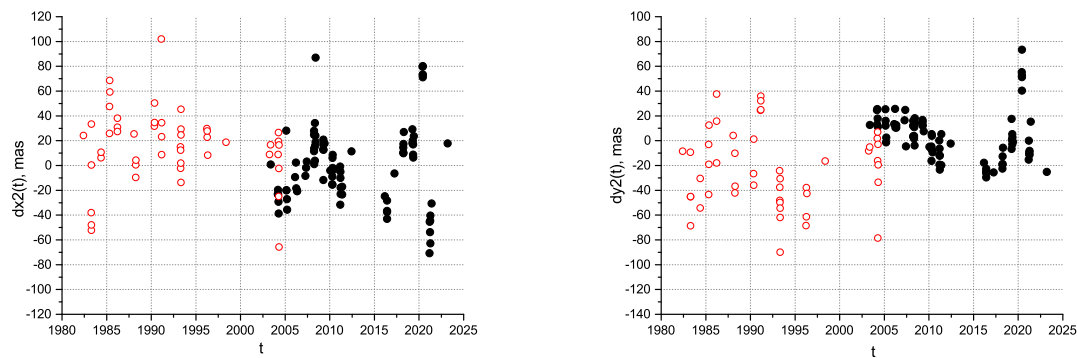


Figure 7: Residual deviations of Pulkovo photographic (red open circles) and CCD (black circles) observations after taking into account both orbits: AB and Ba-Bb.

then an outside observer would most likely find a period of 60 years (the influence of Jupiter and Saturn).

Thus, this question remains open for now. The CCD observations with the 26-inch refractor are continued. Also radial velocity observations and high-precision speckle-interferometric observations of the star ADS 9173 are needed.

References

- Bakos G. A.* Spectroscopic orbital elements of kappa2 Bootis B. // *AJ*. VI 1986. 91. 1416–1417.
- Bally John, Ginsburg Adam, Probst Ron, Reipurth Bo, Shirley Yancy L., Stringfellow Guy S.* Outflows, Dusty Cores, and a Burst of Star Formation in the North America and Pelican Nebulae // *AJ*. XII 2014. 148, 6. 120.
- Gaia Collaboration* . VizieR Online Data Catalog: Gaia DR3 Part 1. Main source // VizieR Online Data Catalog. V 2022. I/355.
- Gaia Collaboration , Brown A. G. A., Vallenari A., Prusti T., et al* . Gaia Data Release 2. Summary of the contents and survey properties // *A&A*. VIII 2018. 616.
- Grosheva E. A.* Analysis of periodic perturbations in the multiple system ADS 15571 // *Astrophysics*. VII 2006. 49, 3. 397–404.
- Izmailov Igor, Rublevsky Aleksey, Apetyan Arina.* Astrometric observations of visual binaries using 26-inch refractor at Pulkovo Observatory during 2014-2019 // *Astronomische Nachrichten*. X 2020. 341, 8. 762–769.
- Kiselev A. A., Kiyaveva O. V.* The Method of Apparent Motion Parameters, used to determine the orbit elements of a visual double star on the basis of short arc observations. // *Astron. Zh. USSR*. 1980. 57, 6. 1227–1241.
- Kiselev A. A., Kiyaveva O. V., Izmailov I. S., Romanenko L. G., Kalinichenko O. A., Vasil'kova O. O., Vasil'eva T. A., Shakht N. A., Gorshanov D. L., Roschina E. A.* Pulkovo catalog

of relative positions and motions of visual double and multiple stars from photographic observations with the 26-inch refractor in 1960-2007 // *Astronomy Reports*. II 2014. 58, 2. 78–97.

Kiyaveva O. V. Using time-distant observations to refine the orbit of a visual double star obtained by the Apparent Motion Parameters method on the basis of a short arc. // *Astron. Zh. USSR*. 1983. 60, 6. 1208–1216.

Kiyaveva O. V. Astrometric study of the triple star ADS 9173 // *Astronomy Letters*. XII 2006. 32, 12. 836–844.

Kiyaveva Olga V., Khovritchev Maxim Yu., Kulikova Agrippina M., Narizhnaya Natalya V., Vasilyeva Tatyana A., Apetyan Arina A. Does ADS 9346 have a low-mass companion? // *Research in Astronomy and Astrophysics*. XII 2021. 21, 11. 291.

Kiyaveva Olga V., Zhuchkov Roman Ya. Dynamical investigations of the multiple stars // *Open Astronomy*. XI 2017. 26, 1. 64–71.

Mason B.D., Wycoff G.L., Hartkopf W.I., Douglass G.G., Worley C.E. The Washington Visual Double Star Catalog. III 2016. Washington: US Naval Observatory, VizieR Online Data Catalog. 0.

Mugrauer M. Search for stellar companions of exoplanet host stars by exploring the second ESA-Gaia data release // *MNRAS*. XII 2019. 490, 4. 5088–5102.

Tokovinin Andrei. The Updated Multiple Star Catalog // *ApJS*. III 2018. 235, 1. 6.

Zakhozhay V. A., Gnedin Yu. N., Shakht N. A. Contributions of the Pulkovo and Kharkiv Scientific Schools to the search for exoplanets and low-mass dark satellites of stars // *Astrophysics*. XII 2010. 53, 4. 575–591.

Table 3: CCD observations of the AB pair with a 26-inch refractor, and residuals.

t, yr	$\rho, ''$	$Err\rho, ''$	$\theta, ^\circ$	$Err\theta, ^\circ$	dx1, mas	dy1, mas	dx2, mas	dy2, mas
2003.380	13.5683	.0034	235.6699	.0158	003.4	022.2	-2.8643	11.8928
2004.180	13.5949	.0056	235.7695	.0179	-029.5	029.6	-26.0504	22.9184
2004.188	13.5987	.0065	235.7208	.0258	-026.1	017.9	-22.5598	11.2674
2004.215	13.5951	.0066	235.7719	.0263	-029.9	030.1	-26.0534	23.6356
2004.259	13.6049	.0067	235.7595	.0161	-036.2	022.2	-31.8589	16.0161
2004.264	13.6166	.0095	235.7579	.0363	-045.7	015.4	-41.3033	9.2484
2005.111	13.5634	.0068	235.6285	.0230	018.1	023.1	29.1807	23.4550
2005.146	13.6108	.0057	235.6954	.0277	-029.9	009.6	-18.7407	10.2505
2005.149	13.6085	.0065	235.7087	.0216	-029.7	013.5	-18.5350	14.1763
2005.206	13.6245	.0083	235.6631	.0186	-036.7	-004.3	-25.4676	-3.1448
2005.217	13.6294	.0060	235.6965	.0202	-045.1	-000.5	-33.8633	0.7470
2006.102	13.5856	.0041	235.6209	.0128	003.7	012.6	-2.8461	14.7308
2006.195	13.5662	.0118	235.6348	.0418	018.1	026.6	8.2601	27.2435
2006.233	13.5908	.0060	235.6320	.0143	-001.7	012.3	-12.7180	12.3128
2006.329	13.5896	.0077	235.6457	.0211	-002.3	016.0	-15.8055	14.4550
2006.348	13.5901	.0053	235.6378	.0210	-001.5	014.2	-15.4203	12.3570
2007.268	13.5794	.0101	235.6586	.0168	007.2	027.6	-9.5144	17.4873
2007.344	13.5705	.0090	235.6742	.0302	012.8	036.0	-3.3668	25.6276
2007.421	13.5840	.0067	235.5621	.0177	016.9	006.7	1.3460	-3.8875
2008.229	13.5697	.0042	235.5838	.0188	028.1	021.9	21.1669	11.4492
2008.240	13.5859	.0048	235.5840	.0159	014.7	012.9	7.9001	2.4767
2008.243	13.5652	.0067	235.5900	.0144	031.1	025.8	24.3371	15.3844
2008.248	13.5794	.0055	235.6090	.0188	016.8	021.5	10.0979	11.0972
2008.259	13.5945	.0049	235.6109	.0174	004.1	013.3	-2.4685	2.9257
2008.327	13.5695	.0073	235.5259	.0229	036.3	011.1	30.5618	0.9155
2008.330	13.5934	.0106	235.6055	.0248	005.9	013.1	0.1978	2.9242
2008.357	13.5800	.0082	235.6017	.0204	017.6	020.1	12.2305	10.0064
2008.390	13.5821	.0047	235.5308	.0182	025.4	005.2	20.4359	-4.7888
2008.406	13.5181	.0094	235.4576	.0167	088.1	027.1	83.3330	17.1639
2008.409	13.5766	.0087	235.6056	.0172	020.0	022.9	15.2705	12.9740
2009.266	13.5954	.0051	235.6201	.0090	005.1	018.3	10.5631	12.7980
2009.269	13.5878	.0088	235.6081	.0181	013.0	020.2	18.4956	14.7187
2009.272	13.5918	.0049	235.6135	.0132	008.9	019.0	14.4268	13.5387
2009.283	13.6174	.0119	235.6701	.0391	-019.7	015.7	-14.0569	10.3139
2009.296	13.5974	.0064	235.6123	.0143	004.6	015.6	10.3806	10.3037
2009.414	13.5975	.0064	235.5814	.0207	008.9	010.0	15.8776	5.5402
2010.058	13.6291	.0064	235.5714	.0171	-013.9	-007.6	-2.7263	-6.8822
2010.279	13.6385	.0061	235.5878	.0160	-023.2	-008.8	-12.2681	-6.2679
2010.282	13.6399	.0084	235.5330	.0291	-017.0	-020.4	-6.0811	-17.8450
2010.285	13.6398	.0119	235.5815	.0277	-023.4	-010.8	-12.4950	-8.2212
2010.299	13.6153	.0089	235.5714	.0338	-001.7	001.1	9.1377	3.7865
2010.318	13.6138	.0054	235.5598	.0159	001.0	-000.3	11.7341	2.5319
2010.323	13.6289	.0057	235.5452	.0146	-009.4	-011.6	1.3046	-8.7303
2010.413	13.6310	.0087	235.5362	.0331	-009.6	-014.2	.3985	-10.6868
2011.161	13.6035	.0113	235.5275	.0279	016.4	002.3	4.6962	1.9170
2011.178	13.6394	.0084	235.5331	.0169	-014.0	-016.9	-26.1629	-17.5611
2011.183	13.6134	.0050	235.4954	.0156	012.6	-009.5	0.3057	-10.2428
2011.186	13.6142	.0060	235.5270	.0243	007.7	-003.8	-4.6734	-4.5925
2011.205	13.6233	.0052	235.5266	.0120	000.3	-009.0	-12.5489	-10.0986

t, yr	$\rho, ''$	$Err\rho, ''$	$\theta, ^\circ$	$Err\theta, ^\circ$	dx1, mas	dy1, mas	dx2, mas	dy2, mas
2011.208	13.6340	.0076	235.4989	.0213	-004.8	-020.4	-17.7232	-21.5477
2011.385	13.6159	.0087	235.6037	.0312	-003.4	011.0	-19.5765	7.2251
2011.388	13.6249	.0046	235.5024	.0180	002.8	-014.0	-13.4149	-17.8143
2012.423	13.5989	.0100	235.5258	.0311	024.0	009.0	9.2995	-1.7953
2016.166	13.6530	.0060	235.4977	.0222	-005.9	-013.9	-20.0280	-15.8974
2016.409	13.6636	.0116	235.5154	.0342	-016.3	-015.5	-33.7144	-20.7763
2016.415	13.6681	.0071	235.4936	.0169	-017.1	-022.3	-34.5598	-27.6451
2016.417	13.6586	.0062	235.4841	.0141	-008.0	-018.8	-25.4743	-24.1675
2016.420	13.6699	.0053	235.5244	.0160	-022.7	-017.3	-40.1967	-22.7023
2017.242	13.6471	.0054	235.4595	.0130	007.2	-014.2	-8.2459	-24.8191
2018.236	13.6478	.0076	235.4464	.0204	011.3	-013.6	6.8038	-23.4619
2018.241	13.6426	.0126	235.4479	.0361	015.3	-010.3	10.8655	-20.1446
2018.247	13.6429	.0064	235.4819	.0224	010.5	-003.8	6.1395	-13.6239
2018.255	13.6403	.0046	235.4431	.0154	018.0	-010.0	13.7390	-19.7956
2018.299	13.6257	.0101	235.4655	.0171	027.1	002.8	23.3820	-6.8365
2019.257	13.6352	.0094	235.5623	.0293	008.9	019.8	16.2159	15.5971
2019.263	13.6398	.0079	235.4516	.0236	020.2	-004.5	27.5728	-8.6587
2019.287	13.6436	.0065	235.4984	.0238	010.8	002.7	18.3991	-1.2797
2019.325	13.6439	.0058	235.5202	.0156	007.6	006.9	15.5475	3.2062
2019.328	13.6553	.0078	235.5116	.0234	-000.6	-001.3	7.3750	-4.9706
2019.350	13.6544	.0053	235.5357	.0201	-003.1	004.1	5.0708	0.5969
2019.410	13.6431	.0047	235.4814	.0199	013.8	000.0	22.4849	-3.0383
2020.404	13.5664	.0108	235.4975	.0384	077.6	050.2	84.8754	54.6701
2020.409	13.5818	.0127	235.4658	.0458	069.3	035.3	76.4714	39.7860
2020.412	13.5731	.0137	235.5021	.0291	071.6	047.4	78.7096	51.8950
2020.415	13.5740	.0081	235.4988	.0266	071.3	046.2	78.3446	50.7040
2020.418	13.5554	.0096	235.5583	.0339	078.6	068.3	85.5816	72.8125
2021.177	13.7096	.0073	235.5911	.0148	-050.8	-009.8	-66.7591	-13.3571
2021.185	13.6800	.0082	235.5847	.0145	-025.5	005.7	-41.5702	2.0328
2021.231	13.6926	.0095	235.5688	.0267	-033.6	-004.4	-50.2398	-8.6746
2021.248	13.6842	.0099	235.5518	.0392	-024.3	-002.9	-41.1256	-7.3920
2021.264	13.6802	.0097	235.5465	.0364	-020.2	-001.6	-37.1874	-6.2911
2021.267	13.7003	.0106	235.5885	.0331	-042.5	-004.7	-59.5158	-9.4272
2021.395	13.6584	.0077	235.6091	.0289	-010.4	023.4	-28.3202	17.2279
2023.205	13.6656	.0053	235.3938	.0173	017.9	-016.6	14.2069	-26.2290

The residuals in right ascension (dx1) and declination (dy1) after taking into account the AMP orbit of the AB pair are used as initial data to determine the astrometric orbit of Ba-Bb. The residuals dx2 and dy2 remain after taking into account also the astrometric Ba-Bb orbit.

Table 4: Orbital elements of the Ba-Bb pair.

	a_{ph}, mas	a, AU	P, yr	e	$\omega, ^\circ$	$i, ^\circ$	$\Omega, ^\circ$	T, yr	M_{Ba}, M_\odot	M_{Bb}, M_\odot	Reference
	18.3	3.56	4.904	.53	82	109	251	2010.917	1.4	≥ 0.48	This work
\pm	3.1	-	-	-	15	14	10	-	-	-	
	*21.3	-	4.904	.53	96	-	-	1927.583	-	≥ 0.5	Bakos (1986)
\pm	3.3	-	0.009	.09	3	-	-	0.016	-	-	

Here: a_{ph} is the semi-major axis of the photocenter orbit, a is the semi-major axis of the relative orbit. * according to (Bakos, 1986) $a_{ph} * \sin(i) = 1$ au, we recalculated the a_{ph} value taking into account the Gaia DR3 parallax (Gaia Collaboration, 2022), the inclination, and its error.